A Comparative Analysis of EEG Network Construction Strategies for Discriminating PNES

Ilaria Lazzaro[1 [0009−0007−1612−2538] ⋆] , Valeria Popello[1 [0009−0004−9273−6935] ⋆], Chiara Zucco[1 [0000−0003−0048−0457]], Marianna Milano[2 [0000−0003−1561−725X]], Antonio Gambardella[3 [0000−0001−7384−3074]], and Mario Cannataro[1 [0000−0003−1502−2387]]

[1] Data Analytics Research Center and Department of Medical and Surgical Sciences, University "Magna Græcia" of Catanzaro, 88100 Catanzaro, Italy
[2] Department of Experimental and Clinical Medicine, University "Magna Græcia" of Catanzaro, 88100 Catanzaro, Italy
[3] Institute of Neurology and Department of Medical and Surgical Sciences, University "Magna Græcia" of Catanzaro, 88100 Catanzaro, Italy {ilaria.lazzaro, valeria.popello, chiara.zucco, m.milano, a.gambardella, cannataro}@unicz.it

Abstract. Network-based EEG analysis has recently attracted attention as a tool for studying alterations in the functional organisation of the brain associated with neurological conditions such as epilepsy and psychogenic non-epileptic seizures (PNES), which represent a diagnostic challenge due to their clinical similarity to epileptic seizures and the absence of epileptiform activity in EEG recordings. In this work, we propose a systematic framework for the construction and analysis of EEG-based functional brain networks, with the aim of evaluating the impact of phase-based connectivity estimators and graph construction strategies on network topology. Functional connectivity matrices were calculated using the phase lag value (PLV), phase locking index (PLI), and weighted phase locking index (WPLI) across multiple frequency bands. Brain networks were constructed using four binarisation and filtering approaches: median threshold, minimum connected component, minimum spanning tree, and orthogonal minimum spanning tree. Global and local graph-theoretic measures were analysed to characterise network organisation in healthy controls, epileptic patients, and PNES patients. The results demonstrate that methodological choices have a marked impact on network topology and critically affect the sensitivity of graph-theoretical measures in distinguishing between clinical groups.

Keywords: Electroencephalogram (EEG) · Functional connectivity · Networks Analysis · Graph theory.

1 Introduction

Psychogenic non-epileptic seizures (PNES) are events of psychological origin, often associated with stress or traumatic experiences, which can closely resemble

⋆ Lazzaro and Popello contributed equally to this work.

ICCS Camera Ready Version 2026
To cite this paper please use the final published version:
DOI: 10.1007/978-3-032-29924-6_13

epileptic seizures in their clinical manifestation. This similarity poses a significant diagnostic challenge, as patients are often unaware of the non-epileptic nature of their seizures [1]. In this context, electroencephalography (EEG) remains a fundamental tool for investigating brain activity, providing a non-invasive measure of neuronal activity. The EEG signal is non-stationary and is typically analysed within canonical frequency bands, conventionally defined as delta, theta, alpha, beta, and gamma, each associated with specific neurophysiological mechanisms [2]. In epilepsy, seizures are commonly accompanied by pathological EEG signatures, such as spikes or sharp waves, while PNES episodes generally do not present epileptiform discharges. Consequently, the current diagnostic gold standard for PNES is based on prolonged video-EEG monitoring, which integrates electrophysiological recordings. In recent years, the analysis of EEG signals has progressively adopted a network-based paradigm [3, 4], modelling the brain as a graph of interacting regions to investigate functional organisation and dynamical properties of brain activity [5, 6]. Numerous studies have applied this framework to brain disorders, reporting alterations in global and local network topology across multiple frequency bands using phase-based functional connectivity measures such as Phase Locking Value (PLV), Phase Lag Index (PLI), and Weighted Phase Lag Index (WPLI) [7, 8]. Alongside connectivity estimation, the construction of functional brain networks represents a critical methodological step. Different strategies—including fixed or proportional thresholding, minimum spanning tree (MST)-based approaches or Minimum Connected Component (MCC), have been proposed to ensure network comparability and interpretability [9]. Recent works have shown that the choice of binarisation or graph construction method can substantially influence network topology and derived graph metrics [10, 11]. However, most existing studies focus on single clinical populations, and systematic comparisons across epilepsy, PNES, and healthy controls remain scarce. In this context, we propose a systematic framework for the construction and analysis of EEG-based functional brain networks, aimed at evaluating the impact of phase-based connectivity estimators and binarisation strategies on network topology. Functional connectivity matrices are computed using PLV, PLI, and WPLI across multiple frequency bands. In addition to binarised networks, a weighted (non-binarised) functional network is also constructed; however, as these networks are fully connected, they are not considered for the extraction and analysis of graph-theoretical measures. Brain networks are then derived using four graph construction approaches: median thresholding (MED), Minimum Connected Component (MCC), Minimum Spanning Tree (MST), and Orthogonal Minimum Spanning Tree (OMST). Global and local topological measures, including global efficiency, local efficiency, degree, strength, and betweenness centrality, are analysed to characterise network organisation in healthy controls, epilepsy patients, and patients with psychogenic non-epileptic seizures. The rest of this paper is organised as follows. Section 2 presents the materials and methods, while Section 3 outlines the experimental results obtained and discusses the findings. Finally, Section 4 presents the conclusions and future work.

ICCS Camera Ready Version 2026
To cite this paper please use the final published version:
DOI: 10.1007/978-3-032-29924-6_13

2 Materials and Methods

This section describes the methodological framework adopted in the study. After providing a brief description of the dataset and the EEG signal pre-processing pipeline, in detail, the construction of functional connectivity matrices and the procedures used for functional network binarisation are presented.

2.1 Dataset

EEG recordings were collected at the Neurology Unit of the Renato Dulbecco University Hospital, Catanzaro, Italy, from three groups of subjects in resting-state conditions: healthy controls (CNT), patients with psychogenic non-epileptic seizures (PNES), diagnosed through video-EEG evaluation in the absence of ictal activity, and patients with epilepsy (EPI). The acquisition protocol, clinical assessment, and data quality procedures followed the methodological framework previously described in [12].

In particular, for the present study, a balanced cohort of 69 subjects was considered, including 23 individuals for each group (CNT, PNES, and EPI). All procedures were conducted in accordance with the Declaration of Helsinki and approved by the local ethics committee. Signals were acquired using a 19-channel Ag/AgCl montage based on the International 10–20 System (Fp1, Fp2, F3, F4, F7, F8, Fz, C3, C4, Cz, P3, P4, Pz, T3, T4, T5, T6, O1, and O2) with a sampling rate of 256 Hz. Recordings were performed in a dimly lit room with participants seated comfortably, with a duration ranging from 10 to 20 minutes. Given the well-known susceptibility of EEG to physiological and environmental artefacts, the raw traces were first visually reviewed by expert neurologists to identify corrupted segments. An automatic preprocessing stage was subsequently applied, including the detection and removal of amplifier saturation events and severely noisy epochs. The cleaned signals were filtered using a Butterworth band-pass filter (0.1–70 Hz) together with a 50 Hz notch filter to attenuate power-line interference. Afterwards, the data were decomposed into five standard frequency bands—delta (0.5–4 Hz), theta (4–8 Hz), alpha (8–13 Hz), beta (13–30 Hz), and gamma (>30 Hz)—via dedicated digital filters. These band-specific signals constituted the basis for the computation of functional connectivity matrices and for the subsequent comparative framework adopted to evaluate different connectivity construction methods and binarization procedures.

2.2 Connectivity Matrix

Starting from pre-processed EEG signals, we calculated functional connectivity matrices using phase-based synchronisation measures.

These measures were selected to capture functional interactions between EEG channels while minimising spurious correlations arising from volume conduction and the use of a common reference. Specifically, the following connectivity metrics were employed:

ICCS Camera Ready Version 2026
To cite this paper please use the final published version:
DOI: 10.1007/978-3-032-29924-6_13

– **Phase Locking Value (PLV)**: quantifies the degree of phase synchronization between two EEG signals by measuring the temporal stability of their phase difference. The PLV ranges between 0 and 1, with higher values indicating stronger synchronization between signal pairs.
Formally, given two EEG signals $x(t)$ and $y(t)$, the PLV is defined as illustrated in Eq. 1[13].

$$\mathrm{PLV}_{xy} = \left| \frac{1}{T} \sum_{t=1}^{T} e^{j\varphi_{xy}(t)} \right|, \tag{1}$$

where $\varphi_{xy}(t) = \phi_x(t) - \phi_y(t)$ denotes the instantaneous phase difference between the two signals at time sample t, T is the total number of samples, and j is the imaginary unit. Despite its simplicity and widespread use due to its high sensitivity and straightforward interpretability, the PLV is particularly susceptible to zero-lag interactions, which may be partially attributed to volume conduction effects or common source activity rather than true functional interactions [14].
– **Phase Lag Index (PLI)**: evaluates the asymmetry of the distribution of phase differences between two EEG signals by considering exclusively non-zero phase-lag interactions. By ignoring phase differences centered around zero, the PLI reduces the influence of volume conduction and common sources, thereby providing a more robust estimate of the functional interactions of genuine neurophysiological origin [15].
The mathematical definition of PLI is defined in Eq. 2 [16].

$$\mathrm{PLI} = \left| \langle \mathrm{sign}\left(\sin(\phi_x(n) - \phi_y(n))\right) \rangle \right|, \tag{2}$$

where $\langle \cdot \rangle$ denotes temporal averaging.
– **Weighted Phase Lag Index (WPLI)**: it represents an extension of the Phase Lag Index (PLI). In which the contribution of phase differences is weighted according to the magnitude of the imaginary component of the cross-spectrum. This weighting strategy improves the statistical stability of the measure and reduces its sensitivity to noise, thereby providing a more reliable estimate of functional connectivity in EEG data [17].
The WPLI is formally defined as follows in Eq. 3 [18].

$$\mathrm{WPLI}_{xy} = \frac{\left| \frac{1}{N} \sum_{n=1}^{N} \left|\mathrm{Im}\left(S_{xy}^{n}\right)\right| \mathrm{sign}\left(\mathrm{Im}\left(S_{xy}^{n}\right)\right) \right|}{\frac{1}{N} \sum_{n=1}^{N} \left|\mathrm{Im}\left(S_{xy}^{n}\right)\right|}, \tag{3}$$

where $\mathrm{Im}(S_{xy})$ denotes the imaginary part of the cross-spectrum between signals x and y, and $\langle \cdot \rangle$ indicates temporal averaging.

2.3 Functional Network Construction Methods

Once the previously described functional connectivity matrices were obtained, brain networks were constructed by applying different binarisation strategies

ICCS Camera Ready Version 2026
To cite this paper please use the final published version:
DOI: 10.1007/978-3-032-29924-6_13

directly to the connectivity matrices [19], in order to compare alternative representations of network topology and to assess the impact of methodological choices on the extracted graph-theoretical measures. Specifically, binarisation procedures were employed to reduce the dependence of network metrics on the absolute distribution of connectivity weights, and to enable robust and reproducible inter-subject and inter-group comparisons. In this study, the binarisation methods considered include median-based thresholding, the Minimum Connected Component (MCC) criterion, the Minimum Spanning Tree (MST) and the Orthogonal Minimum Spanning Tree (OMST) are all applied to the functional connectivity matrices derived from the phase-based synchronisation measures. Specifically, the techniques for binarisation were employed:

- **Median Thresholding (MED)**: is set to the median connectivity weight in the matrix. Connections with weights exceeding the median are retained, while all remaining connections are discarded. This approach yields networks with comparable density across subjects and reduces the influence of extreme connectivity values [20]. However, it may be sensitive to the underlying distribution of connectivity weights and does not explicitly guarantee network connectedness [21].
- **Minimum Connected Component (MCC)**: determines the lowest connectivity threshold that guarantees the resulting binary network to be fully connected, i.e., that at least one path exists between every pair of nodes [22]. By explicitly enforcing global network connectedness, this method prevents fragmentation into disconnected components and preserves the integrative structure of the network, which is essential for the reliable computation of graph-theoretical measures that assume connected graphs. This adaptive property makes the MCC particularly suitable for EEG-based functional connectivity analyses, where inter-subject variability in overall connectivity strength is pronounced.
- **Minimum Spanning Tree (MST)**: constructs a connected and cycle-free subgraph that links all N nodes using exactly $N - 1$ edges, selected to maximise the overall connectivity strength. By definition, the MST enforces a fixed network density across subjects and groups, thereby eliminating potential confounding effects related to differences in edge density and enabling meaningful topological comparisons. Recent investigations have demonstrated that MST-based representations are effective in capturing disease-related alterations in network organisation, including disruptions in network integration and hub structure in neuropsychiatric and neurodegenerative conditions [23, 24].
- **Orthogonal Minimum Spanning Tree (OMST)**: extends the classical Minimum Spanning Tree (MST) framework by iteratively extracting multiple spanning trees that are mutually orthogonal, i.e., constructed on residual connectivity matrices after the removal of edges selected in the previous step iterations. The final network is obtained by combining these orthogonal trees, thereby progressively increasing network density while preserving strict control over connectedness and sparsity [25].

ICCS Camera Ready Version 2026
To cite this paper please use the final published version:
DOI: 10.1007/978-3-032-29924-6_13

2.4 Network Measures

Topological measures provide a quantitative characterisation of a network's structural organisation by describing how nodes and edges are interconnected. These measures are essential for assessing key properties of complex systems, including efficiency, robustness, and modular organisation, and are particularly relevant for the analysis of biological and brain networks [26, 27]. In this study, both global and local topological measures were computed to comprehensively characterise network organisation at the whole-network and node-specific levels. The measures that we considered are:

- ***Local Efficiency***: quantifies how efficiently information is exchanged among its neighbours when that node is removed.
  In Eq. 4, the mathematical details of the local efficiency are shown.

$$E_{loc} = \frac{1}{n}\sum_{i\in N} E_{loc,i} = \frac{1}{n}\sum_{i\in N} \frac{\sum_{j,h\in N; j\neq i, h\neq i} a_{ij}a_{ih}[d_{jh}(N_i)]^{-1}}{k_i(k_i-1)}, \tag{4}$$

  where $d_{jh}(N_i)$ is the shortest path length between nodes j and h restricted to the subgraph formed by the neighbours of i. Local efficiency reflects the system's ability to sustain efficient information transfer within local clusters [28];
- ***Global Efficiency***: provides an alternative but complementary view of integration.
  In Eq. 5 shows the mathematical formula of global efficiency.

$$E_{glob} = \frac{1}{n}\sum_{i\in N} E_i = \frac{1}{n}\sum_{i\in N} \frac{\sum_{j\in N; j\neq i} d_{ij}^{-1}}{n-1}, \tag{5}$$

  In general, global efficiency is high in networks that maintain short paths even between distant nodes, such as functional brain networks during task activation [29].
- ***Degree***: it is defined as the number of edges connected to node i and the formula is illustrated in Eq. 6.

$$k_i = \sum_{j\in N} a_{ij}, \tag{6}$$

  where N is the set of all nodes in the network, and a_{ij} denotes the presence (1) or absence (0) of an edge between nodes i and j. Nodes with high degree, known as *hubs*, are critical for maintaining network connectivity, while nodes with low degree (*non-hubs*) often play peripheral roles. The collection of all degree values defines the *degree distribution*, an important indicator of network organisation and growth [30].
- ***Strength***: extends the concept of degree to weighted networks by taking into account the magnitude of the connections.
  Node strength is defined as the sum of the weights of all edges connected to node i, as shown in Eq. 7.

ICCS Camera Ready Version 2026
To cite this paper please use the final published version:
DOI: 10.1007/978-3-032-29924-6_13

$$s_i = \sum_{j \in N} w_{ij}, \tag{7}$$

where w_{ij} represents the weight of the edge between nodes i and j, and N is the set of all nodes in the network.
Strength reflects not only the number of connections a node has, but also the strength of these connections.
At the network level, the distribution of node strength provides important information about the organisation and heterogeneity of connection weights, complementing the degree distribution in unweighted graphs [31]

– ***Betweenness Centrality***: quantifies the proportion of shortest paths that pass through a given node.
In particular, Eq. 8 illustrates the mathematical definition of betweenness centrality.

$$b_i = \frac{1}{(n-1)(n-2)} \sum_{h,j \in N; h \neq i, j \neq i} \frac{\sigma_{hj}(i)}{\sigma_{hj}}, \tag{8}$$

where n is the total number of nodes, σ_{hj} is the number of shortest paths between nodes h and j, and $\sigma_{hj}(i)$ is the number of such paths passing through node i. Nodes with high betweenness act as communication bridges and are often critical for information flow in the brain or metabolic networks [32, 33].

3 Results and Discussion

After constructing functional brain networks from EEG connectivity matrices, we proceeded with the analysis by evaluating the global and local topological measures of the resulting networks. This analysis was designed to characterise the organisation of the functional brain network across multiple spatial scales, starting from EEG data from our clinical domain. The main objective of this study is to evaluate how methodological choices in network construction influence network analysis results, both in terms of connectivity metrics (PLI, PLV, WPLI) and binarisation and graph-construction strategies (MED, MST, MCC, OMST). The first set of metrics examined comprises global network measures, with a particular focus on global efficiency shown in Fig. 1; it summarises frequency bands, connectivity estimators, and graph construction strategies. The distributions of global efficiency reveal a strong dependence on both the frequency band and the connectivity matrix used to construct the network. In particular, networks constructed using PLV and WPLI in the alpha and theta bands show greater separation of groups (CNT, PNES, EPI). In contrast, PLI-based networks and gamma-band networks show largely overlapping distributions, suggesting limited discriminatory power of global measures in these configurations. Furthermore, when comparing binarisation and graph construction strategies, additional differences emerge: more conservative approaches, such as Minimum Spanning Tree

ICCS Camera Ready Version 2026
To cite this paper please use the final published version:
DOI: 10.1007/978-3-032-29924-6_13

(MST), tend to produce lower, more compressed global efficiency values, further reducing variability between groups. Conversely, denser and more informative strategies, including MCC and OMST, retain a greater proportion of functional connections and exhibit increased variability in global measures.

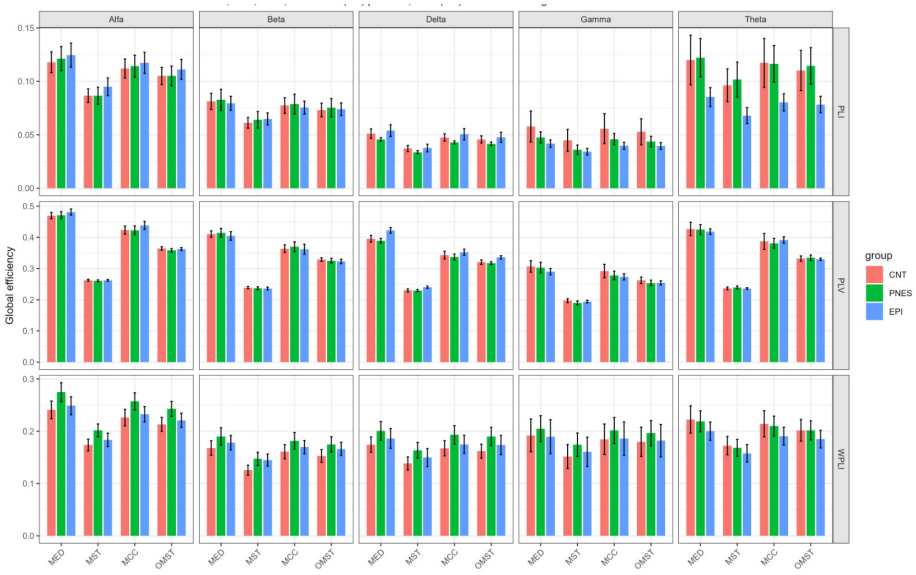

Fig. 1: Global efficiency across frequency bands, connectivity metrics, and graph construction strategies. No statistically significant differences were observed across groups, but results depend on the connectivity metric and graph construction method, with MCC and OMST showing greater variability than MST.

In contrast to global efficiency, local efficiency captures the efficiency of information within the neighbourhood of nodes, providing a measure of local segregation and short-range functional organisation. As shown in Fig. 2, local efficiency is strongly influenced by both the connectivity estimator and the graph construction strategy. Compared to MCC and OMST, MED-based networks exhibit reduced local efficiency values and limited between-group variability, whereas MST-based networks display strongly compressed or near-zero values, reflecting their tree-like topology and the absence of local clustering. In contrast, denser construction strategies such as MCC and OMST preserve local neighbourhood structure and consistently yield higher local efficiency values, particularly when combined with PLV and WPLI in the alpha, beta, and theta bands, where clearer group-level differences can be observed.

ICCS Camera Ready Version 2026
To cite this paper please use the final published version:
DOI: 10.1007/978-3-032-29924-6_13

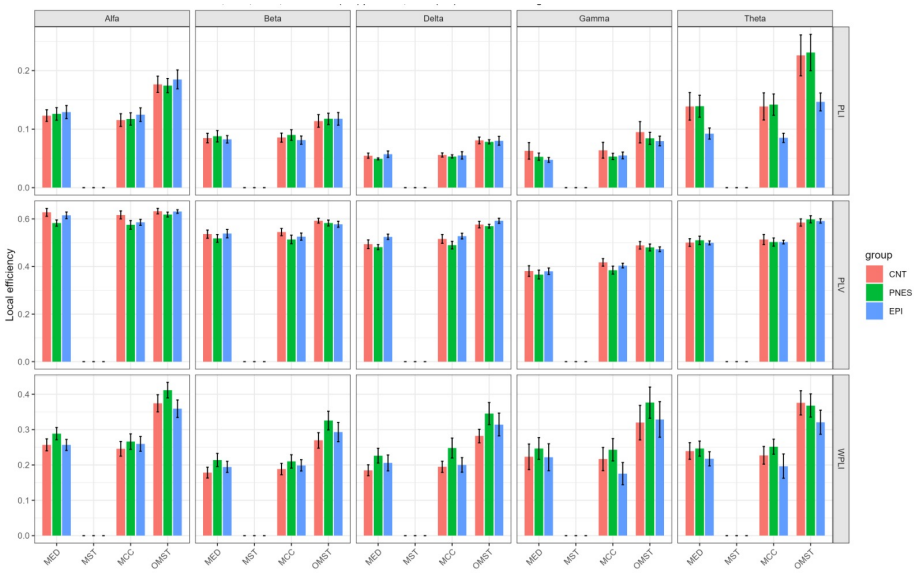

Fig. 2: Local efficiency across frequency bands, connectivity metrics, and graph construction strategies. No statistically significant differences were observed across groups, but MCC and OMST show higher values and variability compared to MED and MST.

Although no statistically significant differences were observed in the joint comparison across the three groups, pairwise analyses revealed significant effects under specific methodological configurations. As shown in Fig. 3, these effects are primarily observed in the delta and theta frequency bands, depending on the graph construction strategy adopted. In particular, the CNT vs PNES comparison did not show statistically significant differences in local efficiency across any of the evaluated configurations. This finding is consistent with previous reports indicating a substantial overlap in EEG-derived functional connectivity patterns between healthy controls and PNES patients, which may limit discriminability at the network level [34]. In contrast, for the CNT vs EPI comparison, significant effects were mainly observed in the delta band, emerging under graph construction strategies that preserve a broader set of connections, such as MED and OMST. In these configurations, EPI networks consistently exhibited higher local efficiency than CNT, suggesting increased local clustering and enhanced short-range information processing. These effects were most pronounced for PLV-based connectivity, indicating that phase synchronisation metrics are particularly sensitive to epilepsy-related alterations in local network organisation. Conversely, no significant differences were detected when MST-based graphs were employed, suggesting that overly sparse network representations may obscure group-specific topological alterations. In the theta band, the CNT vs EPI comparison revealed

ICCS Camera Ready Version 2026
To cite this paper please use the final published version:
DOI: 10.1007/978-3-032-29924-6_13

fewer but still discernible effects, again primarily associated with PLV connectivity combined with OMST filtering. This pattern suggests that theta-band alterations in epilepsy are more subtle and become detectable only when the graph construction strategy balances sparsity with the retention of redundant yet informative connections. A similar trend was observed in the comparison between PNES and EPI, where statistically significant differences emerged under specific graph construction strategies. In particular, with graphs constructed using MED, PNES networks tended to show lower local efficiency than EPI networks, suggesting less local segregation. Conversely, using the MCC strategy, PNES networks showed higher local efficiency than EPI networks, while maintaining the statistical significance of the comparison. This reversal suggests that the differences between PNES and EPI are not unambiguous but critically depend on the filtering criterion adopted, reflecting the varying balance between network density, control of inter-modular connections, and preservation of local topological structure. Overall, the presence of significant effects with both MED and MCC, albeit in opposite directions, suggests that the alterations in local efficiency observed in the PNES vs EPI comparison are sensitive to methodological choices, but at the same time confirms the existence of relevant topological differences between the two clinical conditions.

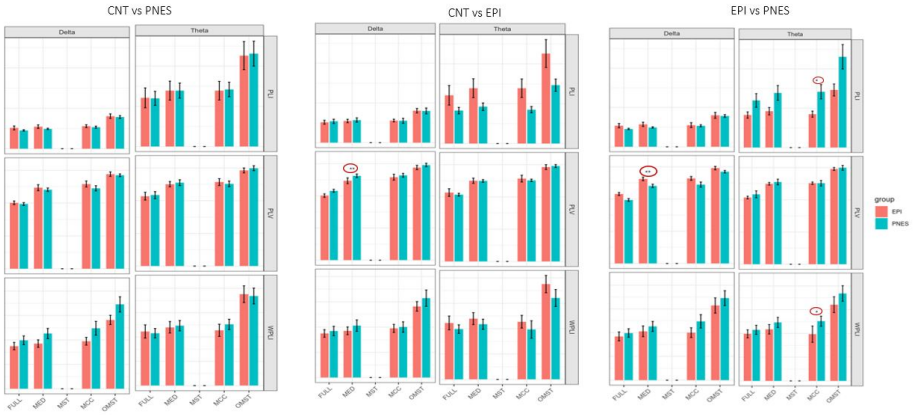

Fig. 3: Pairwise comparisons of local efficiency between clinical groups across delta and theta frequency bands.

After evaluating global efficiency (EG) and local efficiency (EL) across network configurations, the topographical distribution of node degree (node size) and node strength (colour coding) was analysed for all considered cases. Across all graph construction strategies, PLV-based networks exhibit higher and more spatially homogeneous degree and strength values. This behaviour reflects the sensitivity of PLV to zero-lag synchronisation, which tends to produce denser network representations. In contrast, PLI and WPLI yield more conservative and

ICCS Camera Ready Version 2026
To cite this paper please use the final published version:
DOI: 10.1007/978-3-032-29924-6_13

spatially heterogeneous nodal patterns. When comparing binarisation strategies, OMST-based networks show a marked reduction in redundant connections while preserving structurally meaningful hubs. This effect is particularly evident for the OMST–PLI 4a and OMST–WPLI 4b configurations, EPI subjects tend to exhibit increased nodal strength in specific regions, consistent with enhanced local synchronisation, whereas CNT and PNES display more distributed connectivity patterns.

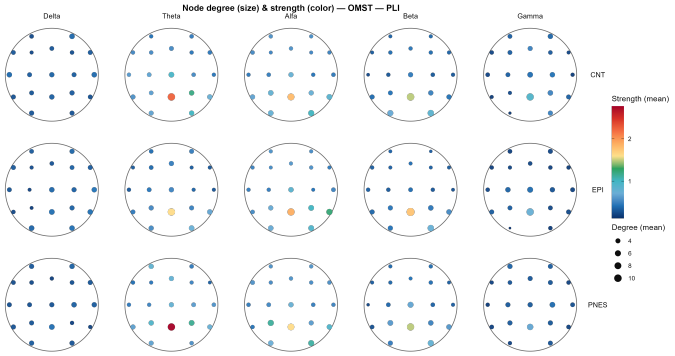

(a) OMST–PLI

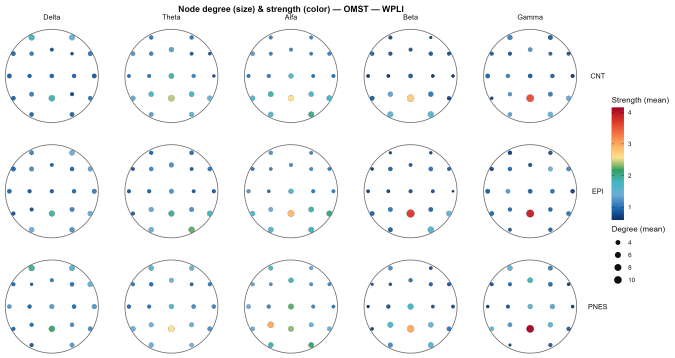

(b) OMST–WPLI

Fig. 4: Topographical distribution of node degree (node size) and node strength (colour) for OMST-based networks constructed using PLI (a) and WPLI (b).

In addition, we also calculated betweenness centrality (BC) to reflect the topological role of a node within the network structure. In fact, PLV-based networks tend to generate dense networks due to their sensitivity to zero-delay synchronisation and have an inflated number of hubs. The PLI configuration par-

ICCS Camera Ready Version 2026
To cite this paper please use the final published version:
DOI: 10.1007/978-3-032-29924-6_13

tially mitigates this problem by discarding zero-delay interactions. In contrast, WPLI does not introduce additional information but removes spurious connections to a sufficient extent to make the betweenness centrality interpretable. The betweenness centrality (BC) measure was calculated to characterise the topological role of each node within the network structure. Topographic maps of BC were generated for all connectivity metrics and graph construction strategies; however, Fig 5 shows only the WPLI-based comparison between EPI and PNES, as this configuration showed the most stable and interpretable effects among the filtering methods. Node-level BC values are projected onto the scalp using interpolated topographic maps, with warmer colours indicating higher BC values.

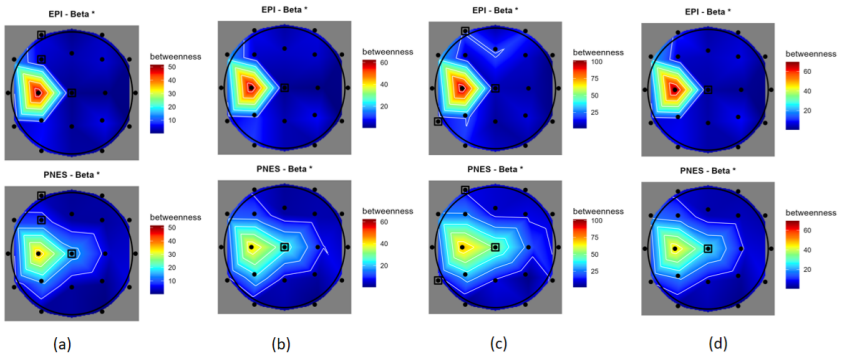

Fig. 5: Topographic maps of betweenness centrality (BC) in the beta band for the WPLI-based EPI vs PNES comparison across different graph construction strategies: (a) WPLI–MED, (b) WPLI–MCC, (c) WPLI–MST, (d) WPLI–OMST.

Specifically, in the WPLI-based comparison between EPI and PNES, the beta band consistently showed statistically significant differences in BC between the MED, MCC, MST and OMST configurations. These differences were visible not only at the global network level but also at the electrode level in the corresponding topographic maps. This convergence between frequency band, connectivity metric, and threshold strategy strongly suggests that the effects observed in the beta band are not determined by a specific filtering choice but are associated with clinical characteristics such as cortical integration, network stabilisation, and maintenance of functional states [34].

4 Conclusions

In this paper, we propose a systematic framework for the construction and analysis of EEG-based functional brain networks, aimed at assessing the impact of

ICCS Camera Ready Version 2026
To cite this paper please use the final published version:
DOI: 10.1007/978-3-032-29924-6_13

connectivity estimators and graph construction strategies on network topology. By combining phase-based connectivity measures (PLI, PLV, WPLI) with multiple binarisation approaches (MED, MCC, MST, OMST), the study highlights how methodological choices substantially influence the resulting network representations. The results indicate that global efficiency alone provides limited discriminative power, while local efficiency and nodal-level analyses offer more informative insights, particularly when denser and data-driven strategies such as MCC and OMST are adopted. Epilepsy-related alterations are more consistently detected in the delta and theta bands, especially when PLV-based connectivity is combined with graph constructions that preserve local clustering. In addition, betweenness centrality contributed to identifying network hubs and communication pathways that differ across clinical groups, providing indications on the reorganisation of information flow within functional brain networks. Despite the encouraging results, this study is limited by the use of a single resting-state EEG dataset and a relatively small sample size. Future work will focus on extending the proposed workflow to larger and more diverse datasets, exploring alternative brain network methodologies, and integrating machine learning approaches to enhance the clinical applicability of EEG-based functional network analysis.

Acknowledgments. This work was funded by the Next Generation EUItalian NRRP, Mission 4, Component 2, Investment 1.5, call for the creation and strengthening of 'Innovation Ecosystems', building 'Territorial R& D Leaders' (Directorial Decree n. 2021/3277)- project Tech4You- Technologies for climate change adaptation and quality of life improvement, n.ECS0000009. This work reflects only the authors' views and opinions, neither the Ministry for University and Research nor The European Commission can be considered responsible for them.

References

[1] Richard J Brown and Markus Reuber. "Psychological and psychiatric aspects of psychogenic non-epileptic seizures (PNES): a systematic review". In: *Clinical Psychology Review* 45 (2016), pp. 157–182.

[2] D Puthankattil Subha et al. "EEG signal analysis: a survey". In: *Journal of medical systems* 34.2 (2010), pp. 195–212.

[3] Marianna Milano et al. "A computational approach to study age-related modifications of the genes involved in Parkinson's disease". In: *Computers in Biology and Medicine* 196 (2025), p. 110765.

[4] Giuseppe Agapito et al. "Ten practical tips and tricks to improve the effectiveness of biological network alignment". In: *PLOS Computational Biology* 21.9 (2025), e1013386.

[5] Ilaria Lazzaro et al. "A Multilayer Network-Based Method for Brain Connectivity Analysis from EEG Data". In: *2024 IEEE International Conference on Bioinformatics and Biomedicine (BIBM)*. IEEE. 2024, pp. 6914–6920.

ICCS Camera Ready Version 2026
To cite this paper please use the final published version:
DOI: 10.1007/978-3-032-29924-6_13

[6] Majid Roshanaei et al. "EEG-based functional and effective connectivity patterns during emotional episodes using graph theoretical analysis". In: *Scientific Reports* 15.1 (2025), p. 2174.
[7] Erick Ortiz et al. "Weighted phase lag index and graph analysis: preliminary investigation of functional connectivity during resting state in children". In: *Computational and mathematical methods in medicine* 2012.1 (2012), p. 186353.
[8] Sergi Abadal et al. "Graph neural networks for electroencephalogram analysis: Alzheimer's disease and epilepsy use cases". In: *Neural Networks* 181 (2025), p. 106792.
[9] Majd Abazid et al. "Weighted brain network analysis on different stages of clinical cognitive decline". In: *Bioengineering* 9.2 (2022), p. 62.
[10] Wan Chen et al. "MDD brain network analysis based on EEG functional connectivity and graph theory". In: *Heliyon* 10.17 (2024).
[11] Narayan Puthanmadam Subramaniyam and Tara C. Thiagarajan. "A novel method for estimating functional connectivity from EEG coherence potentials". In: *Scientific Reports* 15.1 (2025), p. 10723.
[12] Chiara Zucco et al. "Resting-State EEG Classification for PNES Diagnosis". In: *International Conference on Computational Science*. Springer. 2022, pp. 526–538.
[13] Ayan Seal et al. "DeprNet: A deep convolution neural network framework for detecting depression using EEG". In: *IEEE Transactions on Instrumentation and Measurement* 70 (2021), pp. 1–13.
[14] Venkateswarlu Gonuguntla and Jae-Hun Kim. "EEG-based functional connectivity representation using phase locking value for brain network based applications". In: *2020 42nd Annual International Conference of the IEEE Engineering in Medicine & Biology Society (EMBC)*. IEEE. 2020, pp. 2853–2856.
[15] Thanh-Tung Trinh et al. "PLI-Based Connectivity in Resting-EEG is a Robust and Generalizable Feature for Detecting MCI and AD: A Validation on a Diverse Multisite Clinical Dataset". In: *2023 45th Annual International Conference of the IEEE Engineering in Medicine & Biology Society (EMBC)*. IEEE. 2023, pp. 1–6.
[16] Zhiming Wang et al. "Automated rest EEG-based diagnosis of depression and schizophrenia using a deep convolutional neural network". In: *IEEE Access* 10 (2022), pp. 104472–104485.
[17] Laura Sophie Imperatori et al. "EEG functional connectivity metrics wPLI and wSMI account for distinct types of brain functional interactions". In: *Scientific reports* 9.1 (2019), p. 8894.
[18] Baiyang Wang et al. "Depression signal correlation identification from different EEG channels based on CNN feature extraction". In: *Psychiatry Research: Neuroimaging* 328 (2023), p. 111582.
[19] Hye Jeong Jo, Min Jae Lee, and Won Hee Lee. "Graph-theoretical analysis of EEG-based functional connectivity during emotional experience in

ICCS Camera Ready Version 2026
To cite this paper please use the final published version:
DOI: 10.1007/978-3-032-29924-6_13

virtual reality for emotion recognition". In: *Scientific Reports* 15.1 (2025), p. 39965.

[20] Keith Smith, Daniel Abásolo, and Javier Escudero. "Accounting for the complex hierarchical topology of EEG phase-based functional connectivity in network binarisation". In: *PloS one* 12.10 (2017), e0186164.

[21] Bernadette C. M. van Wijk, Cornelis J. Stam, and Andreas Daffertshofer. "Comparing brain networks of different size and density using graph theory". In: *Human Brain Mapping* 31.7 (2010), pp. 1037–1053.

[22] Ramasamy Vijayalakshmi et al. "Minimum connected component–a novel approach to detection of cognitive load induced changes in functional brain networks". In: *Neurocomputing* 170 (2015), pp. 15–31.

[23] Melinda Becske et al. "Minimum spanning tree analysis of EEG resting-state functional networks in schizophrenia". In: *Scientific Reports* 14.1 (2024), p. 10495.

[24] Xing Ye et al. "EEG-based minimum spanning tree analysis reveals network disruptions in Alzheimer's disease spectrum: an observational study". In: *Frontiers in Aging Neuroscience* 17 (2025), p. 1604345.

[25] Timofey Adamovich et al. "The thresholding problem and variability in the EEG graph network parameters". In: *Scientific Reports* 12.1 (2022), p. 18659.

[26] Duncan J Watts and Steven H Strogatz. "Collective dynamics of 'small-world'networks". In: *nature* 393.6684 (1998), pp. 440–442.

[27] Mikail Rubinov and Olaf Sporns. "Complex network measures of brain connectivity: uses and interpretations". In: *Neuroimage* 52.3 (2010), pp. 1059–1069.

[28] Juliana Gonzalez-Astudillo. "Development of Network Features for Brain-Computer Interfaces". PhD thesis. Sorbonne université, 2022.

[29] Vito Latora and Massimo Marchiori. "Economic small-world behavior in weighted networks". In: *The European Physical Journal B-Condensed Matter and Complex Systems* 32.2 (2003), pp. 249–263.

[30] DQ Nykamp. "The degree distribution of a network". In: *Math Insight* (2012).

[31] Alain Barrat et al. "The architecture of complex weighted networks". In: *Proceedings of the national academy of sciences* 101.11 (2004), pp. 3747–3752.

[32] Linton C Freeman. "Centrality in social networks conceptual clarification". In: *Social networks* 1.3 (1978), pp. 215–239.

[33] Marianna Milano, Pietro Hiram Guzzi, and Mario Cannataro. "Network building and analysis in connectomics studies: a review of algorithms, databases and technologies". In: *Network Modeling Analysis in Health Informatics and Bioinformatics* 8.1 (2019), p. 13.

[34] Negar Ahmadi et al. "EEG-based classification of epilepsy and PNES: EEG microstate and functional brain network features". In: *Brain informatics* 7.1 (2020), p. 6.

ICCS Camera Ready Version 2026
To cite this paper please use the final published version:
DOI: 10.1007/978-3-032-29924-6_13